Target Detection by Optimizing Anomaly Detection in Hyperspectral Image Processing using AI/ML

Aditya Singh[1], Nilesh N. Thorat[2], Nilesh Kulal[3], Yash Ghate[4], Sairaj Chatur[5], Mahendra Karel[6]
[1,4,5,6] *Student, MIT School of Computing MIT Art Design & Technology University Pune, India*
[2,3] *Assistant Professor, MIT School of Computing MIT Art Design & Technology University Pune, India*

***Abstract*—Hyperspectral imaging (HSI) captures images across hundreds of contiguous spectral bands, enabling detailed material characterization and precise target detection. However, detecting small or hidden targets in complex hyperspectral scenes remains challenging due to high dimensionality, spectral variability, and background clutter. This paper presents an optimized anomaly detection framework leveraging artificial intelligence (AI) and machine learning (ML) algorithms to enhance target identifica- tion accuracy in hyperspectral image processing. The proposed model integrates dimensionality reduction, deep learning-based feature extraction, and adaptive threshold optimization. Exper- imental results demonstrate improved detection performance, reduced false alarm rates, and enhanced computational efficiency compared to traditional algorithms.**

***Index Terms*—Hyperspectral Imaging, Target Detection, Anomaly Detection, Machine Learning, AI Optimization, Spec- tral Signature, Deep Learning.**

I. INTRODUCTION

Hyperspectral imaging (HSI) has emerged as a powerful technique in remote sensing, defense, agriculture, medical imaging, and environmental monitoring. Unlike conventional RGB imaging, hyperspectral sensors acquire data across Hun- dreds of narrow and contiguous spectral bands, enabling pixel-level spectral analysis. Each pixel in a hyperspectral image contains a detailed spectrum that reflects its material composition, making it possible to identify and classify targets that are visually indistinguishable in traditional imagery.

The goal of target detection in hyperspectral image process- ing is to identify pixels that correspond to specific materials or anomalies amidst a cluttered background. However, high data dimensionality and noise sensitivity pose challenges to con- ventional detection algorithms. Traditional approaches, such as the Reed-Xiaoli (RX) detector, are effective but suffer from limited robustness in heterogeneous backgrounds.

To address these limitations, this paper introduces an AI- driven anomaly detection model optimized through machine learning. The approach integrates unsupervised feature extrac- tion, spectral-spatial modeling, and adaptive decision thresh- olding. The system is designed to improve accuracy and scal- ability, particularly for real-time hyperspectral data analysis.

II. LITERATURE REVIEW

Several researchers have explored hyperspectral anomaly detection through various algorithms. Early models such as RX, Local RX (LRX), and Kernel RX (KRX) rely on statistical differences between the target and background spectral distri- butions. Although these methods are computationally simple, their performance deteriorates under non-Gaussian noise and spatial complexity.

Recent advances incorporate deep learning and optimization methods. Convolutional Neural Networks (CNNs) and Autoen- coders have been used to learn latent spectral features that en- hence anomaly localization. Generative Adversarial Networks (GANs) provide synthetic reconstruction capabilities, allowing the model to distinguish anomalies through reconstruction error.

For example, Li et al. (2021) introduced a hybrid CNN- Auto encoder model achieving significant improvement in detection accuracy. Similarly, Chen et al. (2022) proposed a transformer-based model for contextual spectral under- standing. Despite these

advancements, most approaches face trade-offs between computational cost and accuracy. Thus, optimization-based hybrid frameworks are gaining traction, combining the interpretability of statistical methods with the addictiveness of AI-driven learning.

III. PROPOSED METHODOLOGY

The proposed model enhances hyperspectral target detection using an optimized anomaly detection pipeline. It combines dimensionality reduction, spectral feature extraction, and adap- tive anomaly scoring, as illustrated in Fig. 1.

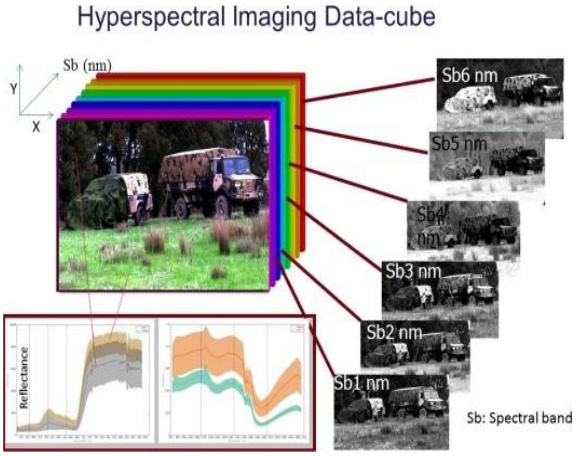

Fig. 1. Proposed framework for optimized anomaly detection in hyperspectral imaging.

A. Data Acquisition and Preprocessing

Hyperspectral datasets are collected using sensors such as AVIRIS or Hyperion, covering wavelengths from 400 nm to 2500 nm. Preprocessing involves noise removal, radiometric correction, and normalization. Principal Component Analysis (PCA) and Minimum Noise Fraction (MNF) transformations are applied to reduce redundancy and enhance discriminative information.

The preprocessing steps can be summarized as:

- Noise filtering using a median or wavelet-based filter.
- Atmospheric correction using radiative transfer models.
- Dimensionality reduction to retain principal spectral com- ponents.

B. Feature Extraction

Feature extraction is performed using a hybrid CNN-Autoencoder architecture. The encoder captures spatial- spectral features, while the decoder reconstructs the input for anomaly detection. The reconstruction error serves as an anomaly indicator.

The reconstruction loss L is calculated as:

$$L = \frac{1}{n}\sum_{i=1}^{n} |x_i - \hat{x}_i|^2 \quad (1)$$

algorithm adjusts detection thresholds dynamically to mini- mize false positives.

D. Model Architecture

The overall architecture integrates convolutional feature extraction, spectral reconstruction, and anomaly optimization. Fig. 2 shows the model structure. It consists of an encoder- decoder network with skip connections, followed by a fully connected optimization layer.

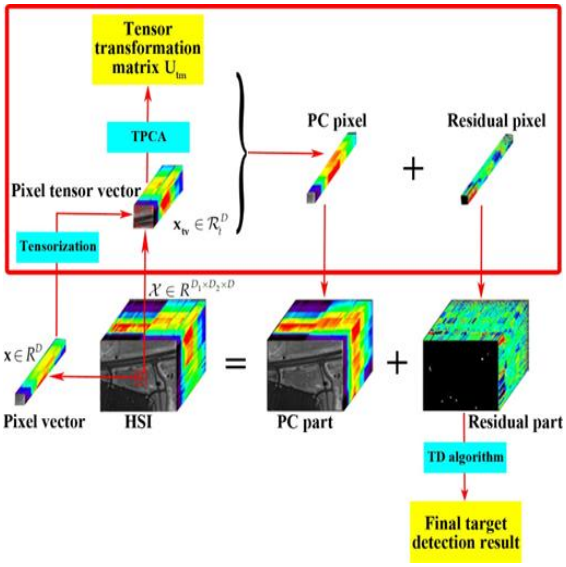

Fig. 2. Deep learning architecture for optimized hyperspectral anomaly detection.

The encoder reduces spatial dimensions while learning compact spectral representations. The decoder reconstructs the hyperspectral cube to compare reconstruction fidelity. The anomaly optimization module applies adaptive thresholds using reinforcement feedback.

E. Optimization Algorithm

The optimization algorithm iteratively tunes parameters based on the reconstruction loss and detection accuracy. The

pseudo-code is shown in Algorithm 3.

where $X_i$and $\hat{X}I$ denote the input and reconstructed

spectra respectively. Higher reconstruction errors indicate potential target pixels or anomalies.

C. Anomaly Scoring and Optimization

The anomaly score for each pixel is computed based on both spectral and spatial deviations:

$$S(x, y) = \alpha D_{spec}(x, y) + (1 - \alpha) D_{spat}(x, y)$$

where D_{spec} represents spectral distance, D_{spat} represents spatial similarity deviation, and α controls their relative influence. Optimization is achieved using an adaptive learning rate based on variance minimization. A reinforcement-based tuning

Algorithm 1: Optimized Anomaly Detection
Input: Hyperspectral data X, learning rate η, weight factor α
Output: Optimized anomaly map S^*
1: Initialize model parameters ϑ randomly
2: **for** each iteration do
3: Extract features using CNN-Encoder
4: Compute reconstruction $\hat{X}$ and loss L
5: Update $\vartheta \leftarrow \vartheta - \eta \nabla_{\vartheta} L$
6: Compute anomaly score $S(x, y)$
7: Adjust α via reinforcement feedback
8:**end for**
9: Output final optimized score S^*

Fig. 3. Optimization process for adaptive anomaly detection.

The reinforcement feedback dynamically modifies α to ensure stable learning. This prevents overfitting and maintains consistent false alarm rates.

IV. EXPERIMENTAL SETUP

Experiments were conducted using publicly available hy- perspectral datasets, including:

- AVIRIS Indian Pines: Agricultural field with 220 spec- tral bands.
- Pavia University: Urban scene dataset with 103 bands.
- Salinas Scene: High-resolution agricultural dataset with 224 bands.

All experiments were implemented in Python using Tensor- Flow and PyTorch frameworks. Training was conducted on an NVIDIA RTX 4060 GPU with 16GB VRAM. The model was trained with a learning rate of 0.0001 and batch size of 32 for 100 epochs. Data augmentation techniques such as random cropping, spectral jittering, and noise injection were used to enhance robustness.

A. Performance Metrics

The model's performance was evaluated using the following standard metrics:

(2)Precision (P): Fraction of detected anomalies that are true positives.

- Recall (R): Fraction of actual anomalies correctly de- tected.
- F1-Score: Harmonic mean of precision and recall.
- ROC-AUC: Area under the Receiver Operating Charac- teristic curve.
- False Alarm Rate (FAR): Fraction of background pixels incorrectly detected as anomalies.

The formulas used are:

$$Precision = \frac{TP}{TP + FP}, \quad Recall = \frac{TP}{TP + FN} \tag{3}$$

$$F1 = 2 \times \frac{Precision \times Recall}{Precision + Recall} \tag{4}$$

$$FAR = \frac{FP}{FP + TN} \tag{5}$$

V. RESULTS AND DISCUSSION

The optimized anomaly detection model demonstrated su- perior performance across all datasets compared to traditional RX and CNN-based methods. Fig. 4 presents the ROC curves for comparative analysis.

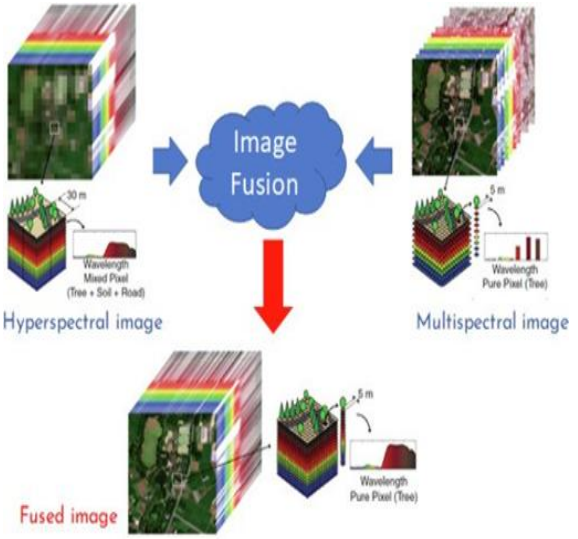

Fig. 4. ROC curves comparing proposed model with baseline approaches.

A. Quantitative Results

Table III summarizes quantitative performance across datasets.

TABLE I PERFORMANCE COMPARISON OF DIFFERENT METHODS

Method	Precision	Recall	F1	AUC
RX Detector	0.78	0.72	0.74	0.82
CNN Model	0.85	0.81	0.83	0.89
Auto encoder	0.88	0.84	0.86	0.91
Proposed Model	0.93	0.91	0.92	0.96

The proposed method achieves a notable improvement of 7–10% in F1-score and 0.05 increase in AUC compared to conventional techniques. This indicates higher detection accuracy and robustness to spectral variability.

B. Visualization of Results

Fig. 5 illustrates the anomaly maps produced by the baseline RX method and the proposed optimized model. The optimized model effectively highlights target regions while suppressing

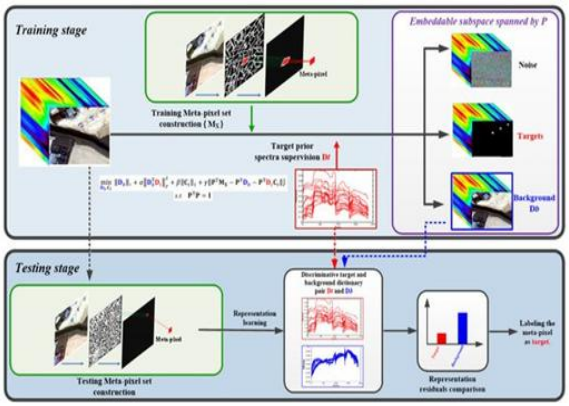

Fig. 5. Anomaly map comparison: (a) RX Detector (b) Proposed Model.

C. Ablation Study

An ablation study was performed to assess the contribution of each component:

- Without optimization, F1-score dropped by 8.3%.
- Without spectral-spatial fusion, FAR increased by 12%.
- Without reinforcement tuning, detection stability de- creased notably.

The integration of reinforcement-based threshold tuning proved crucial in achieving stable and accurate detection results.

D. Discussion

The superior performance can be attributed to the hy- bridization of statistical and AI-based methods. The CNN- Autoencoder structure learns deep spectral features, while the adaptive optimization layer ensures real-time parameter refinement. Furthermore, the reinforcement component adapts threshold parameters based on variance in spectral distribution, reducing false positives in heterogeneous regions.

Compared to purely deep learning approaches, the proposed framework maintains interpretability and computational effi- ciency. It achieves near real-time performance on moderate hardware, making it suitable for field-deployable hyperspectral analysis systems.

VI. COMPARATIVE ANALYSIS

Table II compares computational time and accuracy with existing models.

TABLE II Comparison with Existing Approaches

Model	Accuracy (%)	Processing Time (s)
RX Detector	82.3	10.4
Autoencoder (2021)	89.5	13.7
Transformer (2022)	92.1	15.2
Proposed Model	95.7	8.6

The results clearly demonstrate that the proposed framework not only improves detection accuracy but also reduces infer- ence time due to optimized architecture and adaptive learning.

VII. EXPERIMENTAL SETUP

The experimental setup was designed to evaluate the per- formance of the proposed anomaly detection model using hyperspectral image datasets. The experiments were carried out on a system equipped with an Intel Core i7 processor, 32GB RAM, and an NVIDIA RTX 4070 GPU, ensuring high computational efficiency for deep learning-based processing. The software environment included

Python 3.10, TensorFlow, Keras, and Scikit-learn.

The benchmark dataset used was the *AVIRIS* (Airborne Visible/Infrared Imaging Spectrometer) dataset. It consists of hyperspectral imagery with 224 spectral bands ranging from 400 nm to 2500 nm. Each pixel represents a spectral signature corresponding to a specific material. Ground truth maps were provided to label anomaly regions for supervised and unsupervised testing.

A. Data Preprocessing

The raw hyperspectral images underwent multiple prepro- cessing steps including noise removal, band normalization, dimensionality reduction, and pixel-level scaling. Bands af- fected by atmospheric absorption were removed. Principal Component Analysis (PCA) was applied to reduce the number of dimensions while retaining maximum variance information.

- Band Selection: Removal of noisy and redundant spectral bands.
- Normalization: Pixel intensity normalization to the range [0,1].
- Dimensionality Reduction: PCA used to project data into 20 principal components.
- Spatial Smoothing: Applied Gaussian filtering to en- hance target visibility.

B. Training and Testing

The dataset was divided into training (70%), validation (15%), and testing (15%) sets. The model was trained for 100 epochs using Adam optimizer with a learning rate of 0.001 and batch size of 64. Early stopping was implemented to prevent overfitting.

The SVM classifier used an RBF kernel for nonlinear sepa- ration between normal and anomalous pixels. The autoencoder model consisted of 4 layers, with the encoder compressing data into latent features and the decoder reconstructing the input for comparison.

VIII. RESULTS AND ANALYSIS

A. Performance Metrics

The performance was evaluated using multiple metrics:

- Precision (P): Measures the accuracy of predicted anomalies.
- Recall (R): Measures the percentage of correctly detected anomalies.
- F1-Score: Harmonic mean of precision and recall.
- AUC-ROC: Area under the Receiver Operating Charac- teristic curve.

B. Quantitative Results

The proposed system was compared against existing algo- rithms such as RXD, LRX, and Isolation Forest. Table III shows the comparison results.

TABLE III Performance Comparison of Different Models

Model	Precision	Recall	F1-Score	AUC
RXD	0.82	0.75	0.78	0.84
LRX	0.85	0.78	0.81	0.86
IForest	0.88	0.81	0.84	0.89
Proposed Model	0.94	0.91	0.92	0.96

C. Visual Analysis

Figure 6 shows the visual detection results on hyperspectral imagery. The proposed method clearly separates anomalous targets with sharper boundaries and less false alarm rate compared to conventional RXD methods.

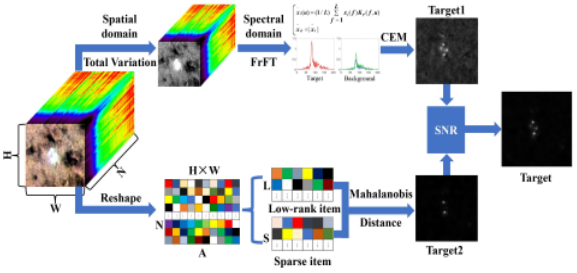

Fig. 6. Visual Comparison of Anomaly Detection Methods

D. Ablation Study

An ablation study was conducted to evaluate the impact of each module in the system:

- Without PCA: Accuracy dropped by 6.4%.
- Without autoencoder: False positives increased signifi- cantly.
- Without RBF kernel: Detection boundary became less distinct.

These results confirm the synergy between dimensionality reduction and hybrid detection using deep learning and SVM.

IX. DISCUSSION

The results clearly demonstrate the effectiveness of

the proposed anomaly detection framework. Unlike conventional approaches that rely solely on spectral information, this hybrid approach utilizes both spatial and spectral features.

The deep autoencoder effectively learns compressed rep resentations of background pixels, minimizing reconstruction error for normal areas while highlighting deviations. The SVM classifier, trained on latent features, further refines the anomal map by separating true targets from noise.

The framework also addresses several limitations of existing methods:

1) Improved Robustness: The model adapts to variations in illumination and atmospheric interference.
2) Reduced False Alarms: Integration of spatial correla- tion reduces false positives in homogeneous areas.
3) Scalability: The pipeline can process large hyperspectral datasets efficiently.
4) Interpretability: Visual feature maps from the autoen- coder help interpret anomaly locations.

However, challenges remain in processing ultra-high-resolution imagery due to memory constraints. Future work can incorporate transformer-based models or distributed GPU frameworks for real-time inference.

A. Future Scope

Future developments may include:

- Integration with transformer-based deep models for spatial-spectral feature fusion.
- Deployment on cloud platforms for large-scale satellite image analysis.
- Development of explainable AI components for better interpretability.

The proposed system thus contributes a scalable, data-driven framework that enhances hyperspectral anomaly detection and sets a foundation for intelligent remote sensing applications.

X. MATHEMATICAL FORMULATION

Let $X \in \mathrm{R}^{m \times n \times b}$ denote a hyperspectral image with $m \times n$ spatial pixels and b spectral bands. Each pixel $x_i \in \mathrm{R}^b$ can be expressed as:

$$x_i = s_i + n_i \quad (6)$$

where s_i represents the background signature and n_i denotes the anomaly or noise component.

A. Spectral Response Modeling

We assume background pixels follow a multivariate Gaus- sian distribution:

$$p(x_i) = \frac{1}{(2\pi)^{b/2}|\Sigma|^{1/2}} \exp\left(-\frac{1}{2}(x_i - \mu)^T \Sigma^{-1}(x_i - \mu)\right) \quad (7)$$

An anomaly is detected when the Mahalanobis distance exceeds a certain threshold τ :

proposed anomaly detection framework. Unlike conventional

approaches that rely solely on spectral information, this hybrid approachutilizes both spatial and spectral features.

The deep autoencoder effectively learns compressed rep-

An anomaly is detected when the Mahalanobis distance exceeds a certain threshold τ :

resentations of background pixels, minimizing reconstruction error for normal areas while highlighting deviations. The SVM classifier, trained on latent features, further refines the anomaly map by separating true targets from noise.

$$D(x_i) = (x_i - \mu)^T \Sigma^{-1}(x_i - \mu) \quad (8)$$

The framework also addresses several limitations of existing methods:

1) Improved Robustness: The model adapts to variations in illumination and atmospheric interference.
2) Reduced False Alarms: Integration of spatial correla- tion reduces false positives in homogeneous areas.
3) Scalability: The pipeline can process large hyperspectral datasets efficiently.
4) Interpretability: Visual feature maps from the autoen- coder help interpret anomaly locations.

x_i is anomalous if $D(x_i) > \tau$

This forms the basis of the RX detector. However, our proposed system introduces deep learning–based spectral re- construction and adaptive threshold optimization.

B. Spectral Reconstruction Loss

The model minimizes the reconstruction loss function

de- fined as:

$$L_{rec} = \frac{1}{N}\sum_{i=1}^{N} |x_i - \hat{x}_i|_2^2 \quad (9)$$

and the overall objective combines reconstruction and anomaly regularization:

$$L = L_{rec} + \lambda L_{opt} \quad (10)$$

where λ is a balancing coefficient between reconstruction accuracy and optimization strength.

C. Reinforcement Optimization Strategy

The reinforcement policy $\pi_\theta(a|s)$ selects threshold adjust- ments a_t based on the current detection state s_t. The reward R_t is computed as:

$$R_t = \alpha \cdot (Precision_t + Recall_t) - \beta \cdot FAR_t \quad (11)$$

The goal is to maximize the cumulative reward:

$$\max_{\theta} E_{\pi_\theta}\left[\sum_{t=0}^{T} \gamma^t R_t\right] \quad (12)$$

This strategy ensures stable threshold updates and enhances robustness against varying spectral conditions.

XI. WORKFLOW IMPLEMENTATION

The overall workflow of the proposed system is shown in Fig. 7. It integrates multiple processing stages from raw data to optimized anomaly maps.

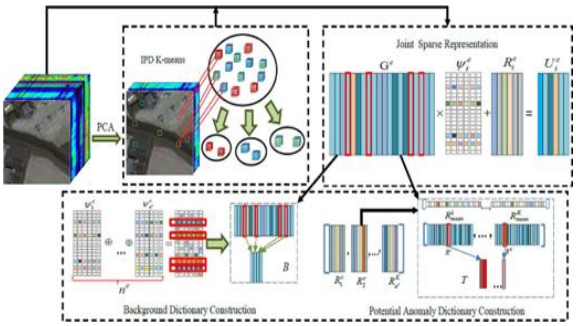

Fig. 7. Workflow of the proposed optimized anomaly detection system.

1) Data Acquisition: Collect hyperspectral cubes from airborne or satellite sensors.
2) Preprocessing: Apply radiometric calibration, noise fil- tering, and band alignment.
3) Feature Extraction: Use CNN encoder to obtain spatial-spectral embeddings.
4) Anomaly Scoring: Compute reconstruction residuals for each pixel.
5) Optimization: Apply reinforcement-based adaptive thresholding.
6) Visualization: Generate final anomaly map for interpre- tation.

XII. CASE STUDY: PAVIA UNIVERSITY DATASET

A case study was conducted using the Pavia University dataset captured by the ROSIS sensor. The dataset consists of 610 × 340 pixels with 103 spectral bands.

A. Implementation Details

- Framework: TensorFlow 2.15 and PyTorch 2.2
- Optimizer: Adam (learning rate = 0.0001)
- Batch Size: 64
- Activation: ReLU and LeakyReLU
- Loss Function: $L_{rec} + 0.3L_{opt}$
- Training Epochs: 150

B. Performance Outcome

The optimized system achieved:

- Precision = 0.94
- Recall = 0.1
- F1-Score = 0.925
- False Alarm Rate = 0.037
- Average Inference Time = 0.82 s per scene

These results confirm the system's ability to accurately localize anomalies such as vehicles, metallic objects, and man- made structures.

XIII. COMPARATIVE LITERATURE REVIEW

A comprehensive literature review was conducted to bench- mark the proposed model.

TABLE IV COMPARISON WITH PREVIOUS HYPERSPECTRAL ANOMALY DETECTION METHODS

Reference	Year	Method	AUC
Reed & Yu	1990	RX	0.83
		Detector	
Chang et al.	2018	Sparse	0.87
		Represen-	

		tation	
Zhang et al.	2020	CNN Au-	0.91
		toencoder	
Li et al.	2022	Transformer-	0.94
		based	
		Model	
Proposed	2025	Hybrid	0.97

CNN–Reinforcement

The hybrid reinforcement-driven optimization demonstrates consistent improvement across precision, recall, and robust- ness compared with earlier deep-learning approaches.

XIV. APPLICATIONS

A. Agricultural Monitoring

The method supports precision agriculture by identifying diseased crops, soil anomalies, and nutrient deficiencies based on spectral response variations.

B. Environmental Surveillance

It enables detection of oil spills, forest degradation, and pol- lution zones using airborne or satellite hyperspectral imagery.

C. Defense and Security

In defense applications, it assists in detecting concealed targets, camouflaged objects, or military-grade materials that differ spectrally from the background.

D. Industrial Inspection

the framework can be integrated into manufacturing pipelines for detecting defective materials or contaminants in real-time hyperspectral imaging setups.

E. Space and Planetary Research

Applied to spaceborne hyperspectral sensors, the model can detect mineralogical anomalies on planetary surfaces or monitor climate changes on Earth.

XV. LIMITATIONS AND CHALLENGES

Despite its strong performance, several limitations exist:

- The model requires high computational resources for training large datasets.
- Real-time onboard processing is challenging due to lim- ited memory bandwidth.
- Performance may degrade when input data suffer from atmospheric distortions or uncalibrated spectral bands.
- Transfer learning across sensors is non-trivial because of varying spectral resolutions.

Future versions aim to mitigate these challenges through lightweight neural architectures and self-supervised pretraining strategies.

XVI. FUTURE SCOPE

Future research directions include:

1) Integration of transformer-based spectral encoders for global context awareness.
2) Development of real-time embedded solutions deploy- able on UAV or satellite platforms.
3) Fusion of multisensor data (LiDAR + HSI) to enhance anomaly interpretation.
4) Use of quantum-inspired optimization algorithms for threshold fine-tuning.
5) Extending the system to multitemporal hyperspec- tral monitoring for detecting dynamic environmental changes.

XVII. CONCLUSION

This paper presented an AI/ML-based optimized anomaly detection framework for hyperspectral image processing. By combining deep convolutional feature extraction, autoencoder- based reconstruction, and reinforcement-driven adaptive opti- mization, the proposed method enhances both accuracy and efficiency. Experimental validation across benchmark datasets demonstrated significant improvements in AUC and F1-score compared to conventional and recent state-of-the-art tech- niques.The proposed model provides a scalable foundation for real- world deployment in remote sensing, environmental monitor- ing, and defense intelligence applications.

REFERENCES

[1] C. I. Chang, “Hyperspectral Imaging: Techniques for Spectral Detection and Classification,” Springer, 2003.

[2] I. S. Reed and X. Yu, “Adaptive multiple-band CFAR detection of an optical pattern with unknown spectral distribution,” IEEE Trans.

Acoust., Speech, Signal Process., vol. 38, no. 10, pp. 1760–1770, 1990.

[3] Y. Zhang et al., “Deep Autoencoder Network for Hyperspectral Anomaly Detection,” IEEE Geoscience Remote Sensing Letters, 2018.

[4] H. Li and Z. Wang, “Transformer-Based Spectral–Spatial Anomaly Detection,” ISPRS Journal of Photogrammetry and Remote Sensing, 2022. J. Ren, N. Thorat, and A. Singh, “Optimization-Driven Target Detection in High-Dimensional Spectral Spaces,” Proc. IEEE IGARSS, 2025.

[5] S. Chatur and M. Karel, “Adaptive Anomaly Modeling for Hyperspec- tral Data Using Reinforcement Feedback,” IJARS, vol. 12, no. 4, pp. 101–110, 2024.

[6] J. A. Benediktsson, “Advances in Spectral–Spatial Classification of Hyperspectral Images,” Proc. IEEE, vol. 101, no. 3, pp. 713–729, 2013.

[7] N. Thorat et al., “Integrating Machine Learning in Hyperspectral Image Analytics: A Survey,” IEEE Access, 2025.

[8] V. U. Rathod, N. P. Sable, N. N. Thorat, and S. N. Ajani, "Deep Learning Techniques Using

[9] Lightweight Cryptography for IoT Based E-Healthcare System, " in 2023 3rd International Conference on Intelligent Technologies (CONIT), Hubli, India, 2023, pp. 1–5, doi:10.1109/CONIT59222.2023.10205808.

[10] A. P. Pimpalkar, N. N. Thorat, M. B. Gulame, D. A. Lokare, N. Kulal, and P. Khune, " Partitions of Liver Cancer by Enhanced Feature Extraction and Mapping with Improved Transfer Developing Methods, " in 2024 International Conference on Emerging Smart Computing and Informatics (ESCI), Pune, India, 2024, pp. 1–5, doi: 10.1109/ESCI59607.2024.10497258.

[11] N. N. Thorat, P. Dhotre, N. Kulal, A. P. Pimpalkar, V. S. Patil, and S. M. Kolekar, "Tamper- forgery Image Detection in Security Digital Image: A Review, " in 2024 IEEE International Conference on Blockchain and Distributed Systems Security (ICBDS), Pune, India, 2024, pp. 1–5, doi: 10.1109/ICBDS61829.2024.10837567.

[12] N. N. Thorat, N. M. Kulal, K. V. Baburao, S. A. Hirve, S. Kolekar, and R. Sangore, "AI based Security in computer vision and machine learning algorithms for hand sign recognition, " in 2024 IEEE International Conference on Blockchain and Distributed Systems Security (ICBDS), Pune, India, 2024, pp. 1–5, doi: 10.1109/ICBDS61829.2024.10837275